

Public-data File 85-26

GEOCHEMICAL INVESTIGATIONS IN THE CHANDALAR C-5 AND C-6  
QUADRANGLES, ALASKA

By

D.D. Adams and J.T. Dillon

Alaska Division of  
Geological and Geophysical Surveys

August 1985

THIS REPORT HAS NOT BEEN REVIEWED FOR  
TECHNICAL CONTENT (EXCEPT AS NOTED IN  
TEXT) OR FOR CONFORMITY TO THE  
EDITORIAL STANDARDS OF DGGS.

794 University Avenue, Basement  
Fairbanks, Alaska 99701

## CONTENTS

	<u>Page</u>
Introduction .....	1
Sampling methods .....	2
Laboratory analysis .....	9
Statistical analysis .....	16
Conclusions .....	20
Discussion .....	25
Acknowledgments .....	27
References cited .....	27
Appendix 1 - Table of analytical results for 1319 stream-sediment samples .....	30
2 - Table of analytical results for 323 pan-concentrate samples .....	30
3 - Summary and graphical statistics for stream-sediment samples .....	30
4 - Summary and graphical statistics for pan-concentrate samples .....	32
5 - Linear correlation coefficients for selected elements of stream-sediment sample data .....	33
6 - Linear correlation coefficients for selected elements of pan-concentrate data .....	34

### FIGURES

Figure 1. Example of prepared sample data sheet .....	3
2. Map showing Ni-Cr and Ni*-Cr* stream-sediment sample distributions .....	5
3. Map showing Ba-B and Ba*-B* stream-sediment sample distributions .....	6
4. Map showing As, and As* pan-concentrate sample distribution .....	7
5. Map showing Ni-Cr and Ni*-Cr* pan-concentrate sample distribution .....	8

### TABLES

Table 1. Analytical methods used and corresponding detection limits for each element .....	4
2. Stream-sediment and pan-concentrate anomaly threshold selected using the Lepeltier method .....	11
3. Stream-sediment and pan-concentrate anomaly thresholds selected using the Sinclair method .....	13
4. Summarized element correlations for stream-sediment sample data .....	18
5. Summarized element correlations for pan-concentrate sample data .....	19

PLATES

- |       |  |           |
|-------|--|-----------|
| Plate | 1. Map of stream-sediment and pan-concentrate sample locations in the Chandalar C-5 and C-6 Quadrangles, Alaska.....             | In pocket |
|       | 2. Map of the anomalous samples and metals determined using the Lepeltier method, Chandalar C-5 and C-6 Quadrangles, Alaska..... | In pocket |
|       | 3. Map of anomalous samples and metals determined using the Sinclair method, Chandalar C-5 and C-6 Quadrangles, Alaska.....      | In pocket |

## INTRODUCTION

A geochemical investigation of the Chandalar C-5 and C-6 Quadrangles, Alaska was conducted during July and August, 1982 by the Alaska Division of Geological and Geophysical Surveys (DGGGS). Locations of 1,319 stream-sediment and 323 pan-concentrate samples collected by student interns are shown on plate 1. Samples were collected in areas of both rugged and gentle topography exclusive of several broad, glacial valleys. Analytical results for the stream-sediment and pan-concentrate samples are listed in appendices 1 and 2 (respectively). Univariate statistical analyses were computed using the University of Alaska-Fairbanks (UAF), Institute of Water Resources (IWR) Hewlett-Packard (HP) 9845-B micro-computer and are given in appendices 3 and 4. The multivariate correlation analyses were computed using the UAF Fair North DEC VAX-11/780 computer and are given in appendices 5 and 6. Plates 2 and 3 are maps of anomalous sample locations and metals which can be used directly to conduct resource exploration. The study area lies within the upper Royukuk Mining district and is the site of recent exploration activity. Funds for this investigations were provided for the Resource Analysis Capitol Improvements Project.

Previous reports concerning the regional geochemistry and geology are available. Stream-sediment geochemistry in the Chandalar Quadrangle is reported in Marsh and others, 1978a, b, c, d, and e. Selected skarn prospects are discussed in Marsh and Wiltse, 1978 and Deyoung, 1978. Dillon (1982) discussed lode- and placer-gold deposits in the region and their sources. Broggé and Reiser (1964) provide a reconnaissance geologic map of the Chandalar Quadrangle.

## SAMPLING METHODS

Stream-sediment samples were collected near the margins of streams at average spacings of approximately one quarter mile (0.4 km). These samples consisted of approximately one half pound (or .2 kg) of clay- to silt-size material. Pan-concentrate samples were collected at about every fourth stream-sediment sample site. These samples consisted of silt - to sand-size material which was sifted through a one quarter-inch (.635 cm) mesh screen and panned down to approximately one quarter pound (or .1 kg). Each sample was placed in an olefin bag at the sample site and was air-dried before shipment to the laboratory. Prepared sample data sheets (fig. 1) were used to record basic geologic information at each sample site.

## LABORATORY ANALYSIS

Most of the laboratory analyses were provided by the DGGs Assay Laboratory in Fairbanks. Bondar-Clegg, Ltd., Vancouver, B.C. provided all tin, tungsten, and mercury analyses as well as some arsenic, nickel, chromium, boron, and barium analyses (reported separately as As\*, Ni\*, Cr\*, B\*, and Ba\*, respectively). Final analyses were received in September, 1983. Analytical methods and corresponding detection limits for each element are summarized in table 1. Since Ni, Ni\*, Cr, Cr\*, Ba, Ba\*, B, B\*, As, As\*, V, and Sr analyses are not ubiquitous for all sample locations their evaluations should include examination of their distributions. Distribution maps are shown for the Ni-Ni\*-Cr-Cr\* and Ba-Ba\*-B-B\* stream-sediment samples (figs. 2 and 3, respectively) and for the As-As\* and Ni-Ni\*-Cr-Cr\* pan-concentrate samples (figs. 4 and 5, respectively).

SAMPLE NOTES

NO 09202

Sample type:

Stream  Soil \_\_\_\_\_ Rock \_\_\_\_\_ Other \_\_\_\_\_

Project:

Township 33N Range 9W Section 9  
 Elevation 3050 Quad. CH C-6  
 Sampler MAS Date 6-18-82

Observations: tributary  
cross sample taken  
no silt deposits

BACK

STREAM SEDIMENT GEOCHEM SAMPLE INFORMATION

1. LOCATION OF SAMPLE RELATIVE TO CL

bottom

2. SEDIMENT SIZE SAMPLED

A-400 B-silt & clay islet

3. ORGANIC CONTENT OF SAMPLE

A Black w/much organic matter  
 B gray, mixed  
 C light / little organic matter

4. CHANNEL TYPE AND WIDTH

A 1-2' B 3-8' C 6-20' D 20-60' E 60'-  
 F- fordable, UF- Unfordable

5. STREAM PROFILE

A Steep w/many falls, rocky, difficult to get sample  
 B Rapid, few falls, line seos. present as well as boulders, gravel  
 C Shallow, prac. meandering, mainly fine sediment.

6. OUTCROPS OF BEDROCK

A cr. flows on bedrock B bedrock exposed w/in 100' C no bedrock seen

7. TYPE OR BEDROCK EXPOSED

Sediments:	sandstone, conglomerate	graywacke	shale, slate	limestone
Percent:				

Meta:	schist	amph	gneiss	greenstone
Percent:	<u>100</u>			

Igneous:	plutonic	volcanic	dike	
				felsic
				inter
				mafic
Percent:				

Figure 1. Example of prepared data sheet.

Table I Analytical methods and corresponding detection limits for the determination of elements (ppm) except for mercury which is reported in parts per billion concentrate columns labeled As\*, Ni\*, Cr\*, B\*, and Ba\*. Abbreviations: r =

AA = Atomic-absorption spectrophotometry.  
 ICP = Inductively coupled plasma atomic-emission spectrophotometry.  
 D.C. = Direct-current, D.C.-arc, semiquantitative emission spectrophotometry  
 F = Fluorescence spectrophotometry.  
 GVA = Cold-vapor, atomic absorption spectrophotometry.  
 G.O. = Gravimetry  
 L. D.L.(SS) = Lower detection limit for stream-sediment analyses.  
 I. D.L.(CC) = Lower detection limit for pan-concentrate analyses.

	Cu	Pb	Zn	Au	Ag	Mn	Sb	As	As*	Co	Ni	Ni*
AA	X	X	X	X	X	X	X	X	X	X	X	X
ICP			X							X	X	
D.C.												
F												
GVA												
G.O.												
L. D.L.(SS)	1	1	-	0.1	1	1	1	1	1	1	10	10
I. D.L.(CC)	1	1	.2	0.1	1	1	1	1	10	10	10	10

Notes: Due to variations in the detection limits several Ba and Sr stream-sediment analyses (1000 ppm for Ba) or (1000, respectively); some Au pan-concentrate analyses (1

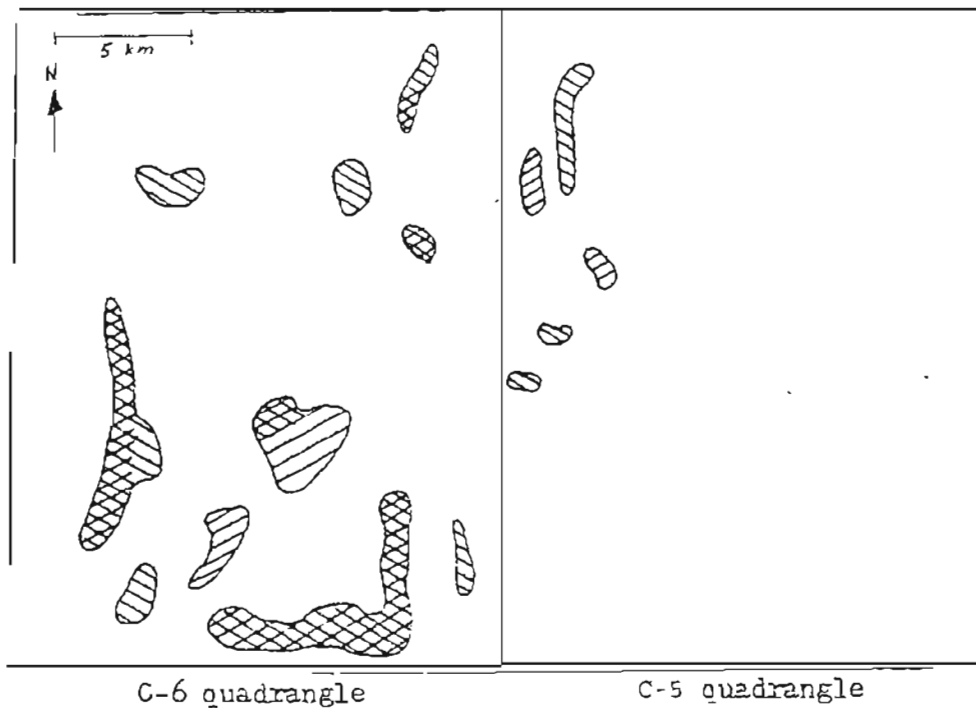

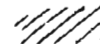



Figure 2. Map showing Ni-Cr- and Ni\*-Cr\*-stream-sediment sample distributions (DGGS and Bondar-Clegg analyses, respectively). Unshaded areas contain sample locations with only Ni and Cr analyses.  = areas containing sample locations with only Ni\* and Cr\* analyses.  = areas containing sample locations with both Ni and Ni\* analyses.  = areas containing sample locations with both Cr and Cr\* analyses. The correlation coefficient for 135 observations with both Ni and Ni\* analyses, 0.9283 (appendix 5), is very high and indicates a significant agreement between these analyses. The linear regression equation for these observations is:  $(Ni^*) = 0.552 + 0.667 (Ni)$ . The correlation coefficient for 98 observations with both Cr and Cr\* analyses, -0.1341 (appendix 5), is effectively random.



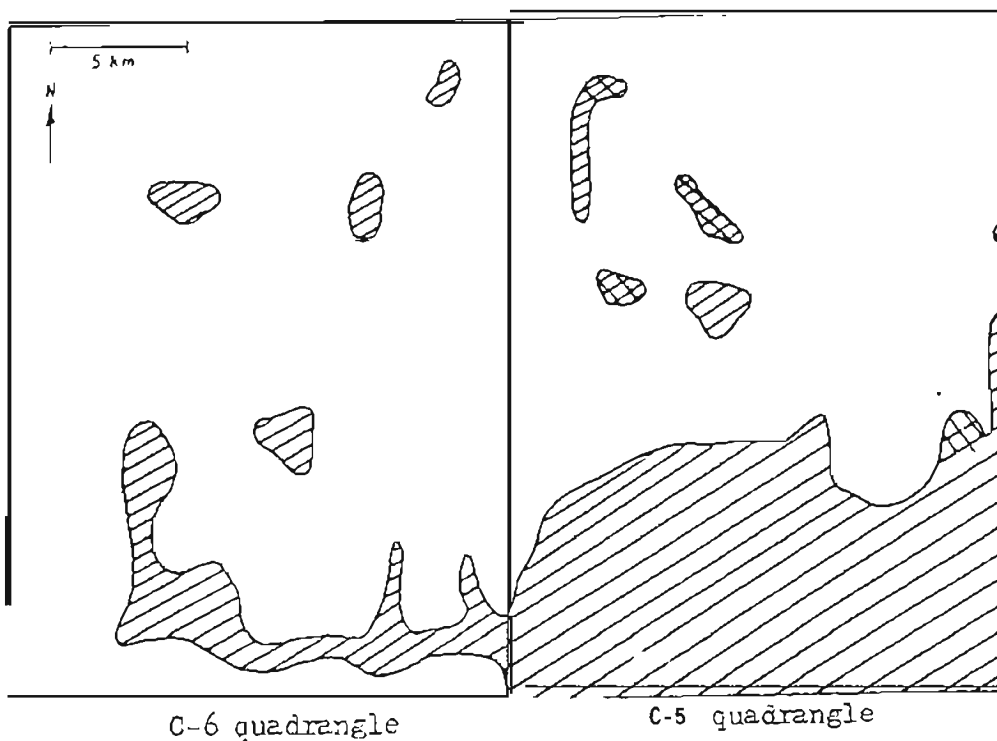


Figure 3. Map showing Ba-B- and Ba\*-B\*-stream-sediment sample distributions (DGS and Bondar-Clegg analyses, respectively). Unshaded areas contain sample locations with only Ba and B analyses.  $\diagdown$  = areas containing samples with only Ba\* and B\* analyses.  $\times$  = areas containing sample locations with Ba, B, Ba\* and B\* analyses. The correlation coefficient for 56 observations with both Ba and Ba\* analyses, 0.628 (appendix 5), is high and indicates a significant agreement between these analyses. The linear regression equation for these observations is:  $(Ba^*) = 208 + 0.029 (Ba)$ . The correlation coefficient for 56 observations with both B and B\* analyses, 0.827 (appendix 5), is high and indicates a significant agreement between these analyses. The linear regression equation for these observations is:  $(B^*) = 21.1 + 0.783 (B)$ .

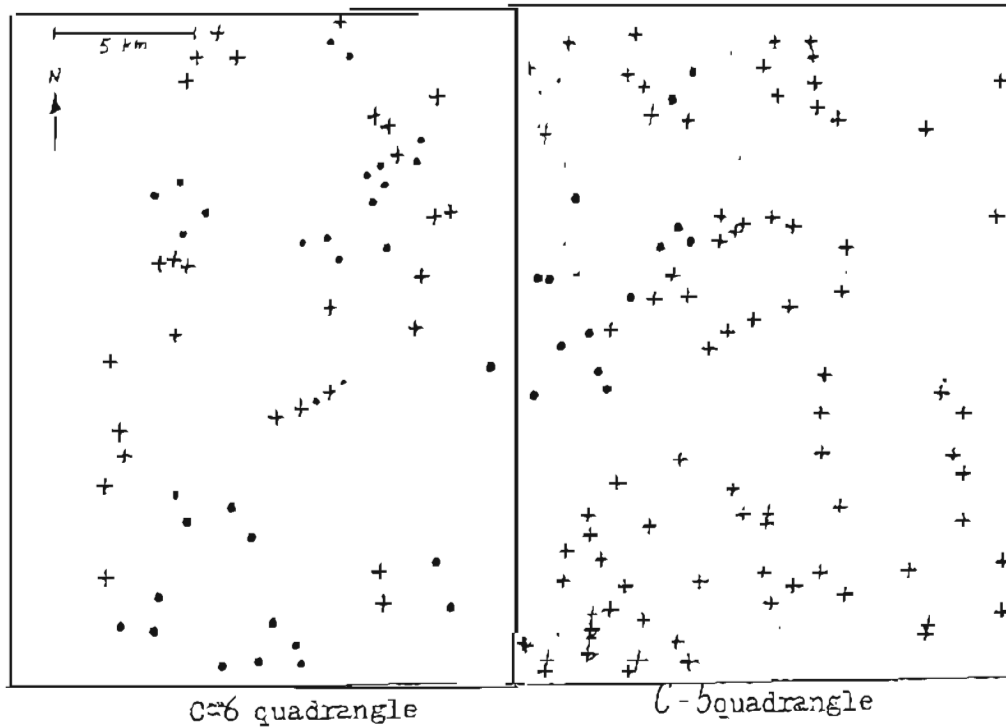


Figure 4. Map showing As- and As\*-pan-concentrate sample distributions (DGGS and Bondar-Clegg analyses, respectively). • = approximate sample location with only an As analyses; + = approximate sample location with only an As\* analysis. All other sample locations (open areas) have both As and As\* analyses. The correlation coefficient for 46 observations with both As and As\* analyses, 0.8851 (appendix 6), is very high and indicates a significant agreement of these analyses. The linear regression equation for these observations is:  $(As^*) = 4.48 + 0.74 (As)$ .

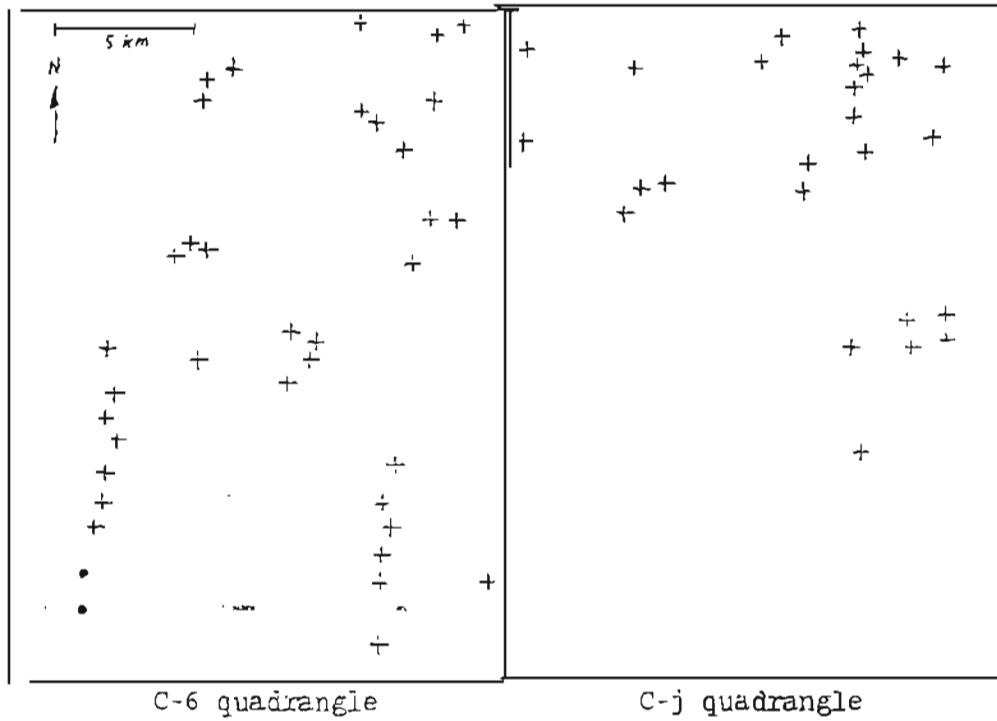


Figure 5. Map showing Ni-Cr- and Ni\*-Cr\*-pan-concentrate sample distributions (DGGs and Bondar-Clegg analyses, respectively). + = approximate sample location with only Ni\* and Cr\* analyses. • = approximate sample location with both Cr and Cr\* analyses. All other sample locations (open areas) have only Ni and Cr analyses.

The DGGG laboratory prepared the samples for analysis by atomic-absorption spectrophotometry (AA) using aqua-regia digestions followed by alliquot extractions with a dilution factor of 1 to 10. Splits of these extractions were diluted again by a factor of 1 to 10 and used for analysis by inductively coupled plasma-emission spectrophotometry (ICP). Bondar-Clegg, Ltd., also used aqua-regia digestions but prepared samples for arsenic analyses using perchloric digestions.

#### STATISTICAL ANALYSIS

Statistical methods are very commonly employed to evaluate large amounts of numerical, geochemical data. These methods are used here to characterize the data, graph frequency distributions and aid in selecting anomaly thresholds. The Ag and Be stream-sediment and Au, Ag, Sb, and Sn pan-concentrate samples were not statistically analyzed because they contain very few unqualified values. The geochemical data were sorted using the IBM Textpack global search system such that qualified (below detection limit) and duplicate analytical values were excluded from the statistical analysis. The data files were then transferred by telephone modem to the HP micro-computer. Log transformations of the values were made to complete the graphical statistics.

Summary statistics for each element consist of basic and order statistics sections and were computed with a 95 percent confidence interval on the mean. Summary statistics of the duplicate analytical values for each element are shown separately. The basic statistics section summarizes the

number of observations, number of missing values, sum, mean, variance, standard deviation, coefficient of skewness, coefficient of kurtosis, coefficient of variation, standard error of the mean and upper and lower limits of the 95 percent confidence interval. The order statistics section lists the maximum and minimum values and corresponding **range**. Midrange and median values and Tukey's hinges and middlemeans are also included in this section. Tukey's hinges are the values of the 25-th and 75-th percentiles and the midspread is the range between these values (J. Tukey, 1977). Tukey's **midmean** is the mean value of the middle 50 percent of the data and can be compared with the regular mean value to estimate the skewness of the data.

Histograms for each element are derived from both the normal and log-transform values (appendices 3 and 4). These are plots of the relative frequency percents typically for 8 to 10 intervals of values. A normal distribution curve is superimposed on the histograms where enough degrees of freedom are available to perform a best fit test.

Cumulative frequency diagrams were obtained using the log transform values plotted on an arithmetic scale. The cumulated frequencies are plotted on the ordinate and the probability is plotted on the abscissa. The statistics program accumulates the frequencies from the lowest to the highest values so the high percentiles correspond to high values for the element.

Initially the cumulative frequency diagrams are treated for threshold selections using the simplified method of iepeltier, 1969. Table 2 lists the

Table 2. Stream-sediment and pan-concentrate anomaly thresholds selected using the method of Lepeltier (1969). The method is a statistical approach which establishes a threshold at the second standard deviation above the mean. Plate 2 is a map showing anomalous sample locations and metals which result from the application of this method. Thresholds for the Ag- and B-stream-sediment and Au-, Ag-, Sb- and Sn-pan-concentrate samples were arbitrarily set at or above their respective detection limits. Thresholds are given in ppm's except that for mercury which is given in ppb's.

	<u>Stream-sediment threshold</u>	<u>Pan-concentrate threshold</u>
CU	71	53
Pb	22	12
Zn	213	141
Ag	0.1	0.1
Mo	8	8
Sb	17	1
AS	92	15
As*		56
co	31	36
Ni	82	79
Ni*	52	58
Fe	62,803	74,097
Mn	2,604	3,633
B	178	125
B*	165	
Ba	823	922
Ba*	1,367	
Cd	6	4
CT	72	482
Cr*	167	38
V	236	
Sr	935	
Be	1	
Sn		5
w		4
Hg	-	86
Au		0.2

- = Not analyzed.

anomaly thresholds selected using this method; plate 2 is the correlative map of anomalous samples, locations, and metals. A single population is generally assumed and anomaly thresholds are selected at the second standard deviation above the mean (or 97.5 percentile intercept). This is the statistical approach to threshold selection suggested by Hawkes and Webb, 1962. Anomaly thresholds for the Pb-, Zn-, and Hg-pan-concentrate samples were selected at slightly lower percentiles which correspond to significant upward breaks in slopes of the frequency curves. Thresholds for the Sb-stream-sediment and As\*-pan-concentrate samples were selected at major inflection points of the curves. Disadvantages of the Lepeltier method are that it tends to give a large number of anomalies due to the inclusion of background with anomalous values and does not distinguish the relative sizes of anomalies.

The cumulative frequency diagrams are also utilized for threshold selections following a partitioning method for polymodal distributions outlined by Sinclair (1974 and 1976). Table 2 and appendices 3 and 4 list the anomaly thresholds, magnitudes and ranges selected using this method; plate 3 is the correlative map of anomalous sample locations and metals. The procedure here involves estimating constituent populations of a distribution and plotting each individual population over the entire probability range. Only populations greater than about 2 probability percent are partitioned. The constituent populations are assigned value ranges which allowed a minimum degree of overlap. Thresholds are then selected at arbitrary percentiles which give a reasonable number of anomalies, defined the relative magnitude of anomalies and limited the inclusion of background values. The Sinclair

Table 3. Stream-sediment and pan-concentrate anomaly thresholds and ranges selected using the method of Sinclair. (1974 and 1976). Thresholds are selected at arbitrary percentiles to establish the anomalies and their relative magnitudes and avoid inclusion of background values. Plate 3 is a map showing anomalous sample locations and metals which result from the application of this method. Types of anomalies are labeled in decreasing order of magnitude as in the following example:

- 1)  $Zn^1$  - threshold set at the 100 percentile of the highest value (A) population,
- 2)  $Zn^2$  - threshold ~~set~~ at the 85 to 98 percentile of the A population,
- 3)  $Zn^3, 4, \text{ etc.}$  - lower limit set at the 90 to 98 percentile of the population and upper limit set at the 0 percentile of the next higher population. A--

Thresholds for the Ag- and Be-stream-sediment and Au-, 'Ag-, Sb-, and Sn-pan-concentrate samples were arbitrarily set at or above their respective detection limits; table 3 and plate 3 shows symbols for these types of values enclosed in parentheses. Thresholds are given in ppm's except that 'for mercury which is given in ppb's.



	Anomaly thresholds	Low level anomaly ranges
Cu-ss cu-pc	$\bar{Cu}^1 = 93, 172, CuCu^2 = 67, 143$	
Pb-ss Pb-pc	$\bar{Pb}^1 = 94, 28 Pb^2 = 67$	
Zn-ss Zn-pc	$Zn^1 =$ $Zn^1 = 471, 228, Zn^2 = 362, 186$	$Zn^3 = 22 \text{ to } 24$
Ag-ss Ag-pc	$(Ag^1) = 0.2 \text{ } 0.7, (Ag) = 0.5$ $(Ag)$	
Mo-ss Mo-pc	$\bar{Mo}^1 = 20, 10, Mo^2 = 9, 17$	
Sb-ss Sb-pc	$Sb^1 = 156, Sb^2 = 71$ $(Sb) = 36$	
As-ss As-pc As*-pc	$As^1 = 133$ $As^1 = 81, As^2 = 60$ $As^2 = 107$	$As^3 = 65 \text{ to } 91$
Co-ss Co-pc	$Co^1 = 199, Co^2 = 111$ $Co^1 = 43$	
Ni-ss Ni-pc Ni*-ss Ni*-pc	$Ni^1 = 193, Ni^2 = 154$ $Ni^1 = 112, Ni^2 = 83$ $Ni^2 = 75$ $Ni^1 = 59$	
Fe-ss Fe-pc	$Fe^1 = 78, 884, Fe^2 = 73, 142$ $Fe^2 = 78, 102$	$Fe^3 = 10,000 \text{ to } 10,998$
Mn-ss Mn-pc	$Mn^1 = 14, 962, Mn^2 = 7, 043$ $Mn^2 = 4, 105$	
B-ss B-pc B*-ss	$B^1 = 231, B^2 = 208$ $B^2 = 209$ $B^1 = 398, B^2 = 339$	$B^3 = 26 \text{ to } 28$
Ba-ss Ba-pc Ba*-ss	$Ba^2 = 933$ $Ba^1 = 1, 220, Ba^2 = 1, 064$ $Ba^2 = 2, 183$	$Ba^3 = 125 \text{ to } 150$
Cd-ss Cd-pc	$Cd^2 = 12$ $Cd^1 = 4$	
Cr-ss	$Cr^1 = 141, Cr^2 = 104$	

Table 3. (con.)

Cr-pc	$Cr^1 = 794, Cr^2 = 479$	$Cr^3 = 179 \text{ to } 254, Cr^4 = 42 \text{ to } 49$
Cr*-ss	$Cr^{*2} = 40178$	
Cr.+pc		
V-ss	$V^1 = 429, V^2 = 331$	
Sr-ss	$Sr^2 = 1,042$	
Sn-pc	$(Sn^1) = 20, (Sn) = 5$	
W-pc	$W^2 = 5$	
Hg-pc	$Hg^2 = 441$	
Au-pc	$(Au) = 0.2$	

method is a more conservative approach but establishes more reliable anomalies and provides a much more detailed analysis of the distribution of values for an element. Low level anomalies which could have local significance can also be identified. Ideally the partitioned populations would correlate with specific lithologies or other geologic features. A complete evaluation of this effect is beyond the scope of this report but more detailed plotting would be encouraged for future studies.

Correlation matrices for the stream-sediment and pan-concentrate data (Appendices 5 and 6, respectively) are computed using the BMDP8D CORPAIR correlation program for incomplete data. This program computes the correlation coefficient between two variables only from cases where unqualified values for both variables are present. The linear correlation coefficients are shown on the lower left half of the tables and the pairwise frequencies with both variables present are shown in the upper right half of the tables. The linear correlation coefficient is a unitless number ranging between +1 and -1 which expresses the relationship between any two variables. A direct relationship or positive correlation of the concentrations of two elements is indicated by a positive coefficient; an inverse relationship is indicated by a negative coefficient. If the correlation coefficient is near zero the relationship between the concentrations of the two elements is random.

### CONCLUSIONS

Considering the sample distributions and generally large number of observations, sample statistics presented here could provide a reasonable base for estimating population parameters. Mean and median values for most

- 1 -

samples are quite similar and could be taken to approximate the population mean. Midrange values often depart significantly from mean and median values especially where wide ranges and large standard deviations are present. Assessment of variance and standard deviations of the samples is difficult due to the polymodal distributions seen for most of the samples.

Most histograms of untransformed values of samples are positively skewed; the lack of skewness in histograms of log transformed values suggests the distributions are lognormal. Polymodal distributions are suggested by the double-peaked histograms of the Sb-stream-sediment 2nd As<sup>+</sup>-, Cr<sup>+</sup>-, and Sa-pan-concentrate samples.

Linear segments forming the curves in most of the cumulative frequency diagrams indicate lognormal distributions. However, the curved form of the log plot and the linear form of the normal plot of the Fe-stream-sediment sample indicates an arithmetic normal distribution (appendix 3). Sample distributions are evaluated 2nd anomaly thresholds are selected by applying statistical 2nd arbitrary graphical methods to the cumulative frequency diagrams. Plotting of anomalies determined by a statistical (Lepeltier) method is useful in outlining regions of anomalous and high background concentrations and distinctive metal associations (pls. 2 and 3). These same geochemical regions are also merked by anomalies determined by another (Sinclair) method which also distinguished their associated anomaly magnitudes.

Significant element correlations for the stream-sediment and pan-concentrate sample data are summarized in tables 4 and 5 (respectively).

Table 4. Significant element correlations determined from coefficients between element pairs for stream-sediment sample data (appendix 5). Correlations based on coefficients beyond critical regions established at a 10% risk level. Very significant positive correlations have coefficients more than one order of magnitude beyond appropriate critical regions.

		Element correlations	
		Very significant positive	Significant negative
			Significant positive
As			Cu, Mo, Pb, Zn
B	B*		Ba, Ba*, Co, Fe, Ni, Pb, V, Zn
Ba	Ba*, V		Co, Cu, Fe, Mo, Ni, Sr, Zn, B
Ba*	Ba		Cd, Co, Cr*, Cu, Mo, Ni, Ni*, Pb, V, Zn
B*	B		Cd, Co, Cr*, Cu, Fe, Mn, Ni, Ni*, Zn
Cd			Co, Cr, Cu, Fe, Mn, Ni, Zn, Ba*, B*
Co	Ni		Cr, Cr*, Cu, Fe, Mn, Ni*, V, Pb, Zn, B, Ba, Ba*, B*, Cd
Cr	Ni		Fe, Ni*, V, Cd, Co
Cr*			Cu, Ni, Ni*, Pb, Zn, Ba*, B*, Co
Cu			Fe, Mo, Ni, Ni*, Pb, Sr, V, Zn, As, Ba, Ba*, B*, Cd, Co, Cr*
Fe			Mn, Ni, Ni*, V, Zn, B, Ba, B*, Cd, Co, Cr, Cu
Mn			Ni, Ni*, Pb, Sr, V, Zn, B*, Cd, Co, Fe
Mo	Zn		Ni, Ni*, Pb, Sr, V, As, Ba, Ba*, Cu
Ni	Zn, Co, Cr		Ni*, Pb, V, B, Ba, Ba*, B*, Cd, Cr*, Cu, Fe, Mn, Mo
Ni*			Pb, Zn, Ba*, B*, Co, Cr, Cr*, Cu, Fe, Mn, Co, Ni
Pb	Zn		V, As, B, Ba*, Co, Cr*
Sr			Ba, Cu, Mn, Mo
V	Zn, Ba		B, Ba*, Co, Cr, Cu, Fe, Mn, Mo, Ni, Pb
Zn	Mo, Ni, Pb, V		As, B, Ba, Ba*, B*, Cd, Co, Cr*, Cu, Fe, Mn, Ni*

Table 5. Significant element correlations determined from coefficients between element pairs for pan-concentrate sample data (appendix 6). Correlations based on coefficients beyond critical regions established at a 10% risk level. Very significant positive correlations have coefficients above an arbitrary cutoff of 0.6.

		Correlation analysis	
		Very significant positive	Significant negative
As	As*		Ni*
As"	As	Cu, Ni	
B	Fe	B, Cu, Pb	Cr, Mo
		Ba, Cd, Co, Cu, Hg, Mn, Ni*, Ni, Pb, Zn, As*	
Ba		Cr*, Cr, Cu, Fe, Mo, Ni*, Pb, Zn,	
Cd		Co, Fe, Mn, Ni, W, Zn, B	Hg
Co	Mn, Ni, Zn	Cu, Fe, Ni*, B, Cd	Mo
Cr*		Pb, Ba	
Cr		Ba	Cu, Fe, Hg, Ni, B
Cu		Fe, Hg, Mn, Ni, Pb, W, Zn, As, As*, B, Ba', Co	Cr
Fe	B	Hg, Mn, Ni, Pb, Zn, Ba, Cd, Co, Cu	Mo, Cr
Hg		Mo, Ni, Zn, B, Cu, Fe	Cd, Cr
Mn	Co	Ni, Zn, B, Cd, Cu, Fe	Mo
Mo		Zn, B a , H g	B, Co, Fe, Mn
Ni*		Pb, Zn, B, Ba, Co	As
Ni	Zn, Co	As, B, Cd, Cu, Fe, Hg, Mn	Cr
Pb		Zn, As*, B, Ba, Cr*, Cu, Fe, Ni*	
W		Cd, Co, Cu	
Zn	Co, Ni	B, Ba, Cd, Cu, Fe, Hg, Mn, Mo, Ni*, Pb	

Coefficients listed in appendices 5 and 6 are classified by establishing critical regions (where  $p = 0$ ) at a 10 percent risk level and selecting the 95 percentile points for the appropriate sample pair frequencies.

Significant positive or negative correlation coefficients are those with values beyond the applied critical regions. Caution must be used to interpret the coefficients due to variable sample pair frequencies, analytical methods (table 1) and geographic sample distributions (figures 2, 3, 4 and 5). For example, a positive Ba-B correlation yet negative Ba-B\* correlation in the stream-sediment data could be explained by differing geographic distributions of the B and B\* samples (figure 2). High positive coefficients between As and As\*, B and B\*, Ba and Ba\* and Ni and Ni\* suggest good agreement between both laboratory analyses. Very strong associations are seen within the assemblage Ni-Cr-V-Pb-Zn-Co for the stream-sediment data. Negative correlations in the stream-sediment data between Mo or Sr and elements which include B, Ba, Cd, Co, Cr, Fe and Mn suggest inverse relationships of their concentrations. The negative correlation of Ni and Cr in pan-concentrates, in contrast to the positive correlation of these in stream-sediments, could be caused by selective occurrence of Cr in detrital accessory minerals.

## DISCUSSION

Five major regions of the study area, distinguished by element associations and geologic features, are outlined on plates 2 and 3. Significant positive correlations (tables 4 and 5) support many of the element associations within the regions. Anomalies outside the selected regions do occur but are not discussed.

## Region I

Region I contains anomalies of Cu, Pb, Zn, As, Sb, Co, Ni, Cr, Ea, Ag, Sn, and W which appear to be directly or indirectly related to coarse-grained, metamorphosed plutonic rocks (pl. 3). Compositions of these rocks range from granite to granodiorite; textures are well foliated and often relict porphyritic. These rocks form the western portions of a belt of plutonic rocks which extends northeastward from region I for approximately 30 km. The northern portion of region I or 'Horace Mt. belt' can be distinguished from the southern portion of this region by its association with anomalous and high background Cu. Cu-Fe-bearing skarns have been observed at the Evelyn Lee and Venus claims (pl. 1) and are reported in Deyoung, 1978. Scattered talc-silicate skarns occur near intrusive contacts throughout region I (pl. 3). Anomalies of As, Sb, Sn, B, Ba, and Co commonly occur downstream from contact zones of the plutons and could be related to skarn, vein, greisen, porphyry or other type of hydrothermal mineralization.

Some of the Ni, Cr, Pb, and Ba anomalies in Region I which are located towards the interiors of the plutonic rock outcrops (or near intrusive contacts) may represent high background levels of these elements from accessory or other minerals which form these rocks. For example, Cr substitutes for  $Fe^{3+}$  in magnetite (Deer and others, 1966) which is known to occur as an accessory in the granitic rocks as well as in some skarns of the region. This speculation is supported by the coincidence of many of the highest (A-population) Cr-pan-concentrate values (appendix 4) with the southern portion of region I (pl. 3). The negative correlation of Cu with Cr



in pan-concentrate samples (table 4) may partly be explained by the spatial separation of high backgrounds of these elements (pl. 3).

## Region II

Region II is a distinctive belt of anomalous Cu occurrences and local Pb, Zn, Mo, As, Ag, Fe, and W anomalies which correspond to a known trend of Cu-bearing talc-silicate skarns (pl. 3). These small skarns typically occur near the contacts of small aplitic or felsic dikes with marble and calcareous schist. Greenschist occurs locally but is seldom associated with significant mineralization. Cu sulfides and hydroxides occur at the Ginger claims (pl. 1) where Cu grades of up to 0.2 percent are reported (Deyoung, 1978). Garnet-idocrase-epidote skarns at the Hurricane-Diane-Luna claims (pl. 1) contain interstitial chalcopyrite, pyrite, tennorite, and cobalt bloom with Cu grades of about 1 percent. Andraditic garnets, which are characteristic of calcic Cu-skarns (Enaudi and others, 1981), have been identified in skarns in both region II and the Horace Mt. belt.

Zn and local Pb, Mo, V, Ba, and Ag anomalies are concentrated in the northwest marginal portion of region II and could be taken to represent the distal portion of a Cu to Zn-Pb geochemical zonation. Although this is a common pattern in many skarn and other hydrothermal systems, Zn-bearing skarns have not been reported from there. A series of greenstone and greenschist bodies just to the west of Region II could also account for the peripheral Zn anomalies (pl. 3). Levinson (1954) suggests plotting of Ni/Co and Ni/Cr ratios can help distinguish between anomaly sources like stratiform

Pb-Zn sulfide mineralization (low Ni/Co ratios) or barren mafic rocks (low Ni/Cr ratios).

Region III

Region III, a broad region in the southern C-5 Quadrangle (pl. 3), contains locally anomalous Zn, Co, Ni, Cr, Ba, Mn, Fe, Pb, W, and Sn. Most of the anomalies in this region occur downstream from cupola zones of metamorphosed granitic stocks compositionally similar to the granitic gneisses of region I. Small skarns are seen locally but significant skarn mineralization has not been found in region III. This may partly be due to the lack of abundant marble or calcareous lithologies. The few skarn occurrences which are known in region III lack associated Cu anomalies in contrast to those of regions I and II. Cupola zones of intrusions commonly form favorable host or source rocks for hydrothermal mineralization like that seen in a vein, greisen, skarn or porphyry environment. The existence of anomalous Sn, Zn, As, Sb, and other elements near the metamorphosed stocks is compatible with these types of mineralization.

Region IV

Anomalous Sb and As ( $\pm$  Zn  $\pm$  Pb) characterize 'region IV' of the study area (pl. 3). A fault zone containing stibnite-quartz vein mineralization with elevated Sb, As, Mo, Hg, Au, and Ag concentrations occurs between marble and graphitic-schist at the south end of Sukakpak Mountain and provides the obvious source of several nearby Sb and As anomalies. Placer gold deposits

are found directly below these veins; many gold placers of the Chandalar and Koyukuk districts are thought to be derived from similar type lodes (Dillon, 1982). Features of some southeast Asian Sb-Ag-Hg deposits, such as localization in fault zones and/or metamorphic rocks and replacement of carbonate lithologies (Hutchinson, 1983), are present at the Sukakpak Mountain locality. Alteration zones associated with the eastern continuation of the fault zone may represent good target areas for future exploration.

#### Region V

Anomalous elements of the suite Zn-Pb-Mo-Co-Ba-B-Mn-V-Ni-Cr characterize the wide, northeast-southwest-trending belt outlined as region V (pl. 3). This belt crudely correlates with a package of distinctive, graphitic, and chloritic quartz schists and phyllite units, and local, thin calcareous or dolomitic schists and marble units. Elsewhere in the Chandalar Quadrangle anomalous Cu, Ba, B, and V are associated with black shale and phyllite of the Hunt Fork Shale Formation and underlying units (Marsh and others, 1978a and c). A principle components analysis of rocks in the Fairbanks district (Hawkins, 1982), which suggests common behaviors of elements within the assemblages Co-Cu-Mn-Ei-Cr-V and Ba-B-Pb-V, agrees with the association of elements in Region V and positive correlations seen among them (tables 4 and 5 and appendices 5 and 6).

The northern portion of region V contains *more* abundant Zn, Mo, Ba, V, and Ni anomalies than the southern portion of the region which contains more abundant B, Mn, Cr, Pb, and Co anomalies. Anomalous Cu is confined to the

central part of the region. The apparent zonation of anomalies may be caused by high backgrounds of selective elements in differing stratigraphic sequences.

The anomalies of Region, V could be formed if stratiform, shale-hosted Pb-Zn or other sediment-hosted deposits were present but mineralization of this type is not known in the area. Favorable characteristics for the presence of these type deposits include the presence of carbonaceous lithologies to serve as host rocks and shale-carbonate facies changes to serve as depositional environments (Gustafson and Williams, 1981).

Some of the Pb, Zn, and Mo anomalies in the eastern portion of region V occur downstream from contacts of graphitic schist with carbonate. Anomalies like these can be caused by the introduction of bicarbonate into stream waters, an increase in pH and consequent metal precipitation (Levinson, 1974).

Samples 449 and 501 contain relatively higher Hg, Pb, and Au backgrounds and are located near a fault. This area should probably be inspected for auriferous Sb-As quartz veins like those observed near Sukakpak Mountain.

#### ACKNOWLEDGMENTS

We wish to thank M.T. Auziller, F.D. Balog, M.S. Lockwood, G. Meyers, M.A. Sturnick, and W.N. Tifental for collecting the samples. DGGs laboratory personnel M.A. Wiltse, T.A. Benjamin, M.R. Ashwell, M.K., Polly, W.W.

Wickens, J.N. Drahos, G.R. Crotty, R.P. Erickson, and J.F. Spielman performed the chemical analyses. We express our thanks to Bub Mueller, Dan Hawkins, and the kind staff of IWR who provided computer facilities, editing, and invaluable advice for this project. Dan Hawkins, Gar Pessel and Kate Ashworth are gratefully acknowledged for critical review of the report. We also thank Penny Adler for drafting assistance and Sunshine Helicopters for logistical support.

#### REFERENCES CITED

- Alaska Division of Geological and Geophysical Surveys, 1982, Mining-claim location maps for the Chandalar Quadrangle, Alaska.
- Brosigé, W.P., and Reiser, H.N., 1964, Geologic map and section of the Chandalar Quadrangle, Alaska: U.S. Geological Survey Map I-375, scale 1:250,000, 1 sheet.
- Dillon, J.T., 1982, Source of lode- and placer-gold deposits of the Chandalar and upper Royukuk districts, Alaska: Alaska Division of Geological and Geophysical Surveys Open-file Report 158, 22 p.
- Deer, W.A., Howie, R.A., and Zussman, J., 1966, Introduction to the rock forming minerals: Longman, London, 528 p.
- Deyoung, J.H., Jr., 1978, Mineral resources map of the Chandalar Quadrangle, Alaska: U.S. Geological Survey Map MF-878-B, scale 1:250,000, 2 sheets.
- Enzudi, M.T., Meinert, L.D., and Newberry, R.J., 1981, Skarn deposits: Economic Geology, 75th Annual volume, p. 317-391.
- Gustafson, L.B., and Williams, N., 1981, Sediment-hosted stratiform deposits of copper, lead, and zinc: Economic Geology, 75th Annual volume, p. 139-178.
- Hawkes, H.E., and Webb, J.S., 1962, Geochemistry and mineral exploration: Harper and Row, 415 p.
- Hawkins, D.B., 1982, Gold content of rocks in the Fairbanks Mining District, Alaska: Alaska Division of Geological and Geophysical Surveys, Open-file Report 168, 103 p.
- Hutchison, C.S., 1983, Economic deposits and their tectonic setting: John Wiley and Sons, New York, 365 p.

Lepeltier, C., 1969, A simplified statistical treatment of geochemical data by graphical representation: Economic Geology, v. 64, p. 538-550.

Levinson, A.A., 1974, Introduction to exploration geochemistry: Applied Pub., Ltd., Calgary, 612 p.

Marsh, S.P., Detra, D.E., and Smith, S.C., 1978a, Geochemical and generalized geologic map showing distribution and abundance of Mo, Cu, and Pb in stream sediments in the Chandalar Quadrangle, Alaska: U.S. Geological Survey Miscellaneous Field Studies Map MF-878 D.

\_\_\_\_\_ 1978b, Geochemical and generalized geologic map showing distribution and abundance of Zn in stream sediments in the Chandalar Quadrangle, Alaska: U.S. Geological Survey Miscellaneous Field Studies M-F-878 E.

\_\_\_\_\_ 1978c, Geochemical and generalized geologic map showing distribution and abundance of Ni, Co, Y, and La in stream sediments in the Chandalar Quadrangle, Alaska: U.S. Geological Survey Miscellaneous Field Studies Map MF-878 F.

\_\_\_\_\_ 1978d, Geochemical and generalized geologic map showing distribution and abundance of Fe, As, B, and V in stream sediments in the Chandalar Quadrangle, Alaska: U.S. Geological Survey Miscellaneous Field Studies Map MF-878 G.

\_\_\_\_\_ 1978e, Geochemical and generalized geologic map showing distribution and abundance of Sb and Pb in stream sediments in the Chandalar Quadrangle, Alaska: U.S. Geological Survey Miscellaneous Field Studies Map MF-878 H.

Sinclair, A.J., 1974, Selection of thresholds in geochemical data using probability graphs: Journal Geochem. Explor., v. 3, p. 129-149.

\_\_\_\_\_, 1976, Applications of probability graphs in mineral exploration:

Association of Explor. Geochemists, spec. v. 4, 95 p.

Tukey, J., 1977, Exploratory data analysis: Addison-Wesley.



APPENDIX 1. Analytical results for 1,319 stream-sediment samples from the Chandalar C-5 and C-6 Quadrangles.

Analytical methods and detection limits are given in table 1. Values are report in parts per million (ppm) except for mercury which is reported in parts per billion (ppb). Qualified values are preceded by '-' (less than) or '+' (greater than) and values not determined are listed as 'nd.' Anomalous values determined from the threshold values listed in table 3 are underlined. Analytical values determined by Bondar-Clegg, Ltd. are reported in separate columns labeled Ni\*, Cr\*, B\*, and Ba\*.

APPENDIX 2. Analytical results for 323 pan-concentrate samples from the Chandalar C-5 and C-6 Quadrangles.

Analytical methods and detection limits are given in table 1. Values are reported in parts per million (ppm) except for mercury which is reported in parts per billion (ppb). Qualified values are preceded by '-' (less than) or '+' (greater than) and values not determined are listed as 'nd.' Anomalous values determined from the threshold values listed in table 3 are underlined. Analytical values determined by Bondar-Clegg, Ltd. are reported in separate columns labeled As\*, Ni\*, Cr\*, B\*, and Ba\*.

APPENDIX 3. Summary and graphical statistical analyses for 1,319 stream-sediment samples from the Chandalar C-5 and C-6 Quadrangles.

Computations for the trace elements use only unqualified valuer end are presented alphabetically. The total number of values used is listed as '#'

observations' or 'number of valid cases.' Summary statistics of the duplicate sample analytical values are shown separately. The symbols Ni\*, Cr\*, B\*, and Ba\* indicate Bondar-Clegg analyses.

Summary statistics are divided into basic and order statistics sections and were computed using a 95 percent confidence interval on the mean. The basic statistics section lists the number of observations, number of missing values, sum, mean, variance, standard deviation, coefficient of skewness, coefficient of kurtosis, coefficient of variation, standard error of the mean and upper and lower limits of the 95 percent confidence interval. The order statistics section lists the maximum value, minimum value, range, midrange, median value, 25th and 75th percentile values (Tukey's hinges), midspread (range between these hinges), midmean (mean of midspread values) and *trimean* (mean of the middle third of the ordered data).

Histograms are plotted using eight to ten intervals of values with the parameters listed. The first histogram is derived from the unqualified values for the element and the second histogram is derived from the log transforms of these values. A normal distribution curve overlay is shown on histograms with sufficient degrees of freedom.

The cumulative frequency diagrams are plots of log transforms on an arithmetic scale. Frequencies are cumulated from the lowest to highest values. The Lepeltier method is used to select thresholds (indicated on the diagrams) and to compile the anomalous samples and elements of plate 2. The Sinclair method is also applied to select thresholds and plot anomalies (pl. 3) and to interpret the distribution of values of each element sample.

Inflection points used for this method are indicated by arrows. Partitioned populations are represented by the line segments labeled A (highest), B, C, etc... followed by their respective percentages (in parentheses). The tables below the diagrams summarize the map symbols, anomaly thresholds, and ranges, estimated population parameters and types of values used in compiling plate 3.

APPENDIX 4. Summary and graphical statistical analyses for 323 pan-concentrate samples from the Chandalar C-5 and C-6 Quadrangles.

Computations for the trace elements use only unqualified values and are presented alphabetically. The total number of values used is listed as '# observations' or 'number of valid cases.' Summary statistics of the duplicate sample analytical values are shown separately. The symbols As\*, Ni\*, Cr\*, B\*, and Ba\* indicate Fondar-Clegg analyses.

Summary statistics are divided into basic and order statistics sections and were computed using a 95 percent confidence interval on the mean. The basic statistics section lists the number of observations, number of missing values, sum, mean, variance, standard deviation, coefficient of skewness, coefficient of kurtosis, coefficient of variation, standard error of the mean and upper and lower limits of the 95 percent confidence interval. The order statistics section lists the maximum value, minimum value, range, midrange, median value, 25th and 75th percentile values (Tukey's hinges), midspread (range between these hinges), midmean (mean of midspread values), and trimean (mean of the middle third of the ordered data).

Appendix 5. Linear correlation coefficients and bivariate frequencies for stream-sediment samples from correlation coefficients between element pairs; upper right half of table lists pairwise frequency element pair computed only from cases for which both elements are present as unqualified values.

	As	B	Ba	Ba*	Bi*	Cd	Co	Cr	Cr*	Cu	Fe
As	--	197	189	187	187	115	339	363	?	383	355
B	0.1163	--	637	56	56	110	636	692	0	697	697
Ba	0.0769	0.2153	--	56	56	84	592	656	0	659	659
Ba*	0.0848	0.4272	0.6280	--	631	203	563	482	230	631	435
Bi*	-0.0160	0.8270	-0.4589	0.0416	--	203	564	483	230	632	496
Cd	0.0512	0.1272	0.0063	0.2268	0.1446	--	273	310	0	314	314
Co	0.0215	0.2797	0.0835	0.0690	0.0802	0.4616	--	1021	230	1161	1025
Cr	-0.0832	-0.0134	0.0426	-0.0185	0.0609	0.2612	0.0712	--	98	1145	1144
Cr*	-0.0600	0.0000	0.0000	0.2770	0.3172	0.0000	0.1469	0.0648	--	230	99
Cu	0.5199	0.0382	0.0992	0.1677	0.1194	0.1501	0.1461	-0.0007	0.2854	--	1158
Fe	0.0267	0.3639	0.1634	-0.0310	0.2469	0.2565	0.3476	0.1711	0.0556	0.1967	--
Mn	-0.0214	0.0247	0.0512	-0.0934	0.0866	0.2483	0.3130	0.0267	-0.0509	0.0345	0.2764
Mo	0.2350	-0.1196	0.2350	0.4325	-0.0757	-0.0064	-0.0423	-0.0570	-0.0891	0.2718	-0.1152
Ni	0.0047	0.1160	0.1824	0.2139	0.0905	0.5290	0.6153	0.5048	0.2634	0.3505	0.2964
Ni*	-0.2572	-0.5685	-0.3405	0.6689	0.3086	0.7474	0.5132	0.2281	0.2854	0.6337	0.5868
Pb	0.4804	0.0888	0.0338	0.2597	0.0181	0.0267	0.1312	-0.0473	0.2302	0.2167	0.0187
Sr	-0.0581	-0.1574	0.2270	-0.3692	-0.5902	-0.2451	-0.1055	-0.0321	0.0000	0.1052	-0.0346
V	0.0430	0.2966	0.2271	0.4277	-0.0274	0.1668	0.2256	0.0791	0.0000	0.1248	0.3965
Zn	0.3851	0.1397	0.4381	0.3788	0.0807	0.4240	0.5063	0.0296	0.1217	0.2136	0.3552

	As	B	Ba	Ba*	Bi*	Cd	Co	Cr	Cr*	Cu	Fe
--	----	---	----	-----	-----	----	----	----	-----	----	----

Appendix 6. Linear correlation coefficients and bivariate frequencies for pan-concentrate samples from I correlation coefficients between element pairs; upper right half of table lists pairwise frequency element pair computed only from cases for which both elements are present as unqualified values.

	As	As*	B	Ba	Cd	co	Cr*	Cu	Fe
As	--	64	209	215	8	215	22	195	315
As*	0.8851	--	64	64	13	63	21	45	64
B	-0.0367	0.2191	--	317	70	308	64	255	317
Ba	-0.0311	-0.1857	0.1617	--	70	314	64	267	323
Cd	0.1070	0.0384	0.2198	-0.1057	--	62	3	67	70
co	0.0970	-0.1118	0.3426	0.0909	0.6912	--	64	252	314
Cr	0.2257	-0.0698	0.0086	0.7711	0.0000	0.0081	--	2	64
Cr*	0.0025	-0.0842	-0.1406	0.3739	0.1157	-0.0270	1.0000	--	761
Cu	0.1964	0.4430	0.4089	0.1583	0.1900	0.2393	0.0149	-0.2021	--
Fe	0.0138	0.0497	0.6108	0.1667	0.3052	0.4053	0.0000	-0.1264	0.3991
Mn	-0.0718	-0.0511	0.1769	0.0725	-0.2039	0.0353	-0.1707	-0.2618	0.1207
Mn	-0.0178	0.1216	0.5927	0.0709	0.5040	0.6408	0.0000	0.0156	0.2949
Mo	0.0700	0.0092	-0.2709	0.1368	-0.1938	-0.1952	0.1063	0.0759	0.0741
Mo	-0.3887	-0.0214	0.4954	-0.4099	-0.0695	0.5633	-0.0253	0.0000	0.1801
NI*	0.1477	-0.1150	0.2448	0.0939	0.5909	0.8606	0.0000	-0.2383	0.2081
NI	0.0847	0.3157	0.1871	0.195%	0.0762	0.0046	0.8135	-0.0788	0.4371
Pb	-0.0263	-0.0831	0.0409	0.0640	0.2133	0.0198	0.1788	0.0991	0.1388
Zn	-0.0561	-0.0406	0.3157	0.3819	0.5371	0.6379	-0.1141	0.0447	0.3787